

# Soluble Yttrium Chalcogenides: Syntheses, Structures, and NMR Properties of $Y[\eta^3\text{-N}(\text{SPPH}_2)_2]_3$ and $Y[\eta^2\text{-N}(\text{SePPh}_2)_2][\eta^3\text{-N}(\text{SePPh}_2)_2]$

Christopher G. Pernin and James A. Ibers\*

Department of Chemistry, Northwestern University, 2145 Sheridan Road, Evanston, Illinois 60208-3113

Received August 16, 1999

The compounds  $Y[\text{N}(\text{QPPH}_2)_2]_3$  (Q = S (**1**), Se (**2**)) have been synthesized in good yield from the protonolysis reactions between  $Y[\text{N}(\text{SiMe}_3)_2]_3$  and  $\text{HN}(\text{QPPH}_2)_2$  in methylene chloride ( $\text{CH}_2\text{Cl}_2$ ). The compounds are not isostructural. In **1**, the Y atom is surrounded by three similar  $[\text{N}(\text{SPPH}_2)_2]^-$  ligands bound  $\eta^3$  through two S atoms and an N atom. The molecule possesses  $D_3$  symmetry, as determined in the solid state by X-ray crystallography and in solution by  $^{89}\text{Y}$  and  $^{31}\text{P}$  NMR spectroscopies. In **2**, the Y atom is surrounded again by three  $[\text{N}(\text{SePPh}_2)_2]^-$  ligands, but two are bound  $\eta^2$  through the two Se atoms and the other ligand is bound  $\eta^3$  through the two Se atoms and an N atom. Although a fluxional process is detected in the  $^{31}\text{P}$  and  $^{77}\text{Se}$  NMR spectra, a triplet is found in the  $^{89}\text{Y}$  NMR spectrum of **2** ( $\delta = 436$  ppm relative to  $\text{YCl}_3$  in  $\text{D}_2\text{O}$ ,  $^2J_{\text{Y-P}} = 5$  Hz). This implies that on average the conformation of one  $\eta^3$ - and two  $\eta^2$ -bound ligands is retained in solution. Crystallographic data for **1**:  $\text{C}_{72}\text{H}_{60}\text{N}_3\text{P}_6\text{S}_6\text{Y}$ , rhombohedral,  $R\bar{3}c$ ,  $a = 14.927(5)$  Å,  $c = 56.047(13)$  Å,  $V = 10815(6)$  Å<sup>3</sup>,  $T = 153$  K,  $Z = 6$ , and  $R_1(F) = 0.042$  for the 1451 reflections with  $I > 2\sigma(I)$ . Crystallographic data for **2**:  $\text{C}_{72}\text{H}_{60}\text{N}_3\text{P}_6\text{Se}_6\text{Y}\cdot\text{CH}_2\text{-Cl}_2$ , monoclinic,  $P2_1/n$ ,  $a = 13.3511(17)$  Å,  $b = 38.539(7)$  Å,  $c = 14.108(2)$  Å,  $\beta = 94.085(13)^\circ$ ,  $V = 7241(2)$  Å<sup>3</sup>,  $T = 153$  K,  $Z = 4$ , and  $R_1(F) = 0.037$  for the 8868 reflections with  $I > 2\sigma(I)$ .

## Introduction

We recently reported the syntheses, structures, and solution properties of a variety of rare-earth imidodiphosphinochalcogenido compounds of the type  $\text{Cp}_2\text{Ln}[\text{N}(\text{QPPH}_2)_2]$  (Ln = Y, La, Gd, Er, Yb; Q = S, Se).<sup>1</sup> In each, the structure in the solid state consists of a  $\text{Cp}_2\text{Ln}$  fragment coordinated either  $\eta^2$  through the two chalcogen atoms of the imidodiphosphinochalcogenido ligand,  $[\text{N}(\text{QPPH}_2)_2]^-$ , or  $\eta^3$  through the two chalcogen atoms and the N atom of the ligand. Various NMR spectroscopies indicated that the solid-state connectivity is retained in solution. The ability of the rare-earth atoms to accommodate the two different coordination modes of the ligand was surprising because the ligand had previously been shown only to exhibit  $\eta^2$ -binding to transition metals.<sup>2–19</sup>

The reaction that produced those compounds is



The limitation of this approach is that regardless of the amount of  $\text{HN}(\text{QPPH}_2)_2$  added, the reaction only proceeds to the monosubstituted complexes or in the case of Ln = La gives a mixture of products. To reach  $\text{LnL}_3$  complexes, a more labile rare-earth starting material is necessary. To this end we have successfully used  $Y[\text{N}(\text{SiMe}_3)_2]_3$ . In this paper we report the syntheses, X-ray crystal structures, and NMR properties of  $Y[\text{N}(\text{QPPH}_2)_2]_3$  (Q = S (**1**), Se (**2**)).

## Experimental Section

**General Procedures.** All manipulations were carried out under strict exclusion of  $\text{O}_2$  and  $\text{H}_2\text{O}$  with the use of standard Schlenk techniques.<sup>20</sup>  $\text{CH}_2\text{Cl}_2$  was distilled from  $\text{P}_2\text{O}_5$  and bubbled with Ar for 10 min before use.  $Y[\text{N}(\text{SiMe}_3)_2]_3$  was synthesized according to a published procedure and stored in an Ar-filled glovebox before use.<sup>21</sup>  $\text{HN}(\text{QPPH}_2)_2$  was synthesized from  $\text{HN}(\text{PPh}_2)_2$  and elemental chalcogen (Q) in a manner similar to published procedures.<sup>11,13</sup> NMR data on  $\text{CD}_2\text{Cl}_2$  solutions of **1**, **2**, and  $\text{HN}(\text{QPPH}_2)_2$  were recorded on either a Gemini 300 MHz

- (1) Pernin, C. G.; Ibers, J. A. *Inorg. Chem.* **1999**, *38*, 5478–5483. Pernin, C. G.; Ibers, J. A. *Inorg. Chem.* **2000**, *39*, 1216–1221.
- (2) Churchill, M. R.; Cooke, J.; Fennessey, J. P.; Wormald, J. *Inorg. Chem.* **1971**, *10*, 1031–1035.
- (3) Rossi, R.; Marchi, A.; Marvelli, L.; Peruzzini, M.; Casellato, U.; Graziani, R. *J. Chem. Soc., Dalton Trans.* **1992**, 435–437.
- (4) Rossi, R.; Marchi, A.; Marvelli, L.; Magon, L.; Peruzzini, M.; Casellato, U.; Graziani, R. *J. Chem. Soc., Dalton Trans.* **1993**, 723–729.
- (5) Balakrishna, M. S.; Klein, R.; Uhlenbrock, S.; Pinkerton, A. A.; Cavell, R. G. *Inorg. Chem.* **1993**, *32*, 5676–5681.
- (6) Haiduc, I.; Silvestru, C.; Roesky, H. W.; Schmidt, H.-G.; Noltemeyer, M. *Polyhedron* **1993**, *12*, 69–75.
- (7) Casas, J. S.; Castiñeiras, A.; Haiduc, I.; Sánchez, A.; Sordo, J.; Vázquez-López, E. M. *Polyhedron* **1994**, *13*, 2873–2879.
- (8) Balakrishna, M. S.; Santarsiero, B. D.; Cavell, R. G. *Inorg. Chem.* **1994**, *33*, 3079–3084.
- (9) Silvestru, C.; Rösler, R.; Haiduc, I.; Cea-Olivares, R.; Espinosa-Pérez, G. *Inorg. Chem.* **1995**, *34*, 3352–3354.
- (10) Bhattacharyya, P.; Woollins, J. D. *Polyhedron* **1995**, *14*, 3367–3388.
- (11) Bhattacharyya, P.; Slawin, A. M. Z.; Williams, D. J.; Woollins, J. D. *J. Chem. Soc., Dalton Trans.* **1995**, 2489–2495.
- (12) Bhattacharyya, P.; Slawin, A. M. Z.; Williams, D. J.; Woollins, J. D. *J. Chem. Soc., Dalton Trans.* **1995**, 3189–3193.
- (13) Bhattacharyya, P.; Novosad, J.; Phillips, J.; Slawin, A. M. Z.; Williams, D. J.; Woollins, J. D. *J. Chem. Soc., Dalton Trans.* **1995**, 1607–1613.

- (14) Cupertino, D.; Keyte, R.; Slawin, A. M. Z.; Williams, D. J.; Woollins, J. D. *Inorg. Chem.* **1996**, *35*, 2695–2697.
- (15) Cea-Olivares, R.; Novosad, J.; Woollins, J. D.; Slawin, A. M. Z.; García-Montalvo, V.; Espinosa-Pérez, G.; García y García, P. *Chem. Commun.* **1996**, 519–520.
- (16) Woollins, J. D. *J. Chem. Soc., Dalton Trans.* **1996**, 2893–2901.
- (17) García-Montalvo, V.; Novosad, J.; Kilian, P.; Woollins, J. D.; Slawin, A. M. Z.; García y García, P.; López-Cardoso, M.; Espinosa-Pérez, G.; Cea-Olivares, R. *J. Chem. Soc., Dalton Trans.* **1997**, 1025–1029.
- (18) Bhattacharyya, P.; Slawin, A. M. Z.; Smith, M. B. *J. Chem. Soc., Dalton Trans.* **1998**, 2467–2475.
- (19) Muñoz-Hernández, M.-A.; Singer, A.; Atwood, D. A.; Cea-Olivares, R. *J. Organomet. Chem.* **1998**, *571*, 15–19.
- (20) Shriver, D. F.; Drezdon, M. A. *Manipulation of Air Sensitive Compounds*, 2nd ed.; Wiley: New York, 1986.
- (21) Wilkinson, G.; Birmingham, J. M. *J. Am. Chem. Soc.* **1954**, *76*, 6210.

spectrometer ( $^{31}\text{P}$  (for **1**) and  $^1\text{H}$  with a 5 mm NMR probe) or a 400 MHz Varian spectrometer ( $^{31}\text{P}$  (for **2**) and  $^{77}\text{Se}$  with a 10 mm broadband NMR probe,  $^{89}\text{Y}$  with a 10 mm low-frequency probe) at 25 °C.  $^{31}\text{P}$  chemical shifts, in ppm, were recorded at 120.470 MHz for **1** and at 161.904 MHz for **2** and were referenced to an external standard of 85%  $\text{H}_3\text{PO}_4$  (set to 0 ppm).  $^{77}\text{Se}$  chemical shifts, in ppm, were recorded at 76.295 MHz and referenced to an external standard of a saturated solution of  $\text{Ph}_2\text{Se}_2$  in  $\text{C}_6\text{D}_6$  (set to 460 ppm).  $^{89}\text{Y}$  chemical shifts, in ppm, were recorded at 19.598 MHz and referenced to an external standard of 3 M  $\text{YCl}_3$  in  $\text{D}_2\text{O}$ . Variable temperature  $^{31}\text{P}$  NMR spectroscopic data on compound **2** were collected from a 0.01 M solution of **2** in  $\text{CD}_2\text{Cl}_2$  with the following parameters: 15 °C, 1000 transients,  $d_1 = 1$  s, pulse width = 15  $\mu\text{s}$ ; -40 °C, 5000 transients,  $d_1 = 1$  s, pulse width = 15  $\mu\text{s}$ .  $^{31}\text{P}$  NMR parameters for **1** were similar to those for **2** though the experiments were carried out at 25 °C.  $^{77}\text{Se}$  NMR collection parameters for **2**: 11 172 transients,  $d_1 = 1$  s, pulse width = 20  $\mu\text{s}$ , 0.04 M solution of **2** in a 1:4 mixture of  $\text{CD}_2\text{Cl}_2/\text{CH}_2\text{Cl}_2$ .  $^{89}\text{Y}$  NMR collection parameters for **1**: 16 465 transients,  $d_1 = 5$  s, pulse width = 15  $\mu\text{s}$ , 0.07 M solution of **1** in  $\text{CD}_2\text{Cl}_2$ .  $^{89}\text{Y}$  NMR collection parameters for **2**: 12 672 transients,  $d_1 = 3$  s, pulse width = 15  $\mu\text{s}$ , 0.04 M solution of **2** in  $\text{CD}_2\text{Cl}_2$ .  $^{89}\text{Y}$  collection parameters and results for  $\text{Y}[\text{N}(\text{SiMe}_3)_2]_3$ : singlet, 563 ppm, 0.04 M solution in  $\text{CD}_2\text{Cl}_2$ ,  $d_1 = 20$  s, pulse width = 20  $\mu\text{s}$ , 249 transients. Melting point determinations were performed with a Mel-Temp device on samples sealed in glass capillaries. Elemental analyses were performed by Oneida Research Services, New York.

$\text{Y}[\text{N}(\text{SPPH}_2)_2]_3$  (**1**). On approximately a 200 mg total scale, in a 1:3 molar ratio white crystalline  $\text{Y}[\text{N}(\text{SiMe}_3)_2]_3$  and white powdered  $\text{HN}(\text{SPPH}_2)_2$  were loaded in separate flasks in an Ar-filled glovebox. The flasks were removed from the box and attached to a Schlenk line where 10 mL of  $\text{CH}_2\text{Cl}_2$  was added to each via syringe. The clear solution of  $\text{HN}(\text{SPPH}_2)_2$  was added via syringe to the clear solution of  $\text{Y}[\text{N}(\text{SiMe}_3)_2]_3$ , and the resulting clear solution was stirred for 1 h. The volume of the solution was reduced to 10 mL, and while sitting overnight at -15 °C, it produced large clear colorless crystals of **1**. Melting point: 210 °C. Yield: 79%. Anal. Calcd for  $\text{C}_{72}\text{H}_{60}\text{N}_3\text{P}_6\text{Se}_6\text{Y}$ : C, 60.29; H, 4.22; N, 2.93. Found: C, 60.26; H, 4.26; N, 2.67.  $^{31}\text{P}\{-^1\text{H}\}$  NMR: 42.5 ppm ( $d$ ,  $^2J_{\text{P-Y}} = 4$  Hz).  $^{89}\text{Y}\{-^1\text{H}\}$  NMR: 284 ppm (multiplet). No absorption is present in the UV/vis spectrum between 230 and 800 nm.

$\text{Y}[\text{N}(\text{SePPh}_2)_2]_3$  (**2**, **2a**). A procedure similar to **1** was used to produce clear crystals of **2**. Cooled, concentrated  $\text{CH}_2\text{Cl}_2$  solutions of **2** produced crystals suitable for the structure determination reported here. This material contains one  $\text{CH}_2\text{Cl}_2$  molecule of crystallization per Y center as determined in the X-ray crystal structure. Methylene chloride solutions of **2** diluted with diethyl ether produced crystals containing one ether molecule per Y center, as deduced from chemical analysis and the crystal structure (compound **2a**).  $^1\text{H}$  NMR spectroscopy on this material also supports the presence of the diethyl ether of crystallization, with peaks at 1.17 ppm (t,  $\text{CH}_3\text{CH}_2$ ) and 3.44 ppm (q,  $\text{CH}_3\text{CH}_2$ ) relative to tetramethylsilane. Melting point of **2**: solid turns orange by 230 °C and turns to a red liquid at 266 °C. Yield: 91%. Elemental analyses were performed on the material isolated from the diethyl ether-diluted solutions (**2a**). Anal. Calcd for  $\text{C}_{72}\text{H}_{60}\text{N}_3\text{P}_6\text{Se}_6\text{Y}\cdot\text{C}_4\text{H}_{10}\text{O}$ : C, 51.0; H, 3.94; N, 2.35. Found: C, 50.87; H, 3.88; N, 2.40.  $^{31}\text{P}\{-^1\text{H}\}$  NMR: 32.4 ppm ( $^1J_{\text{P-Se}} = 580$  Hz;  $^2J_{\text{P-P}} = 28$  Hz).  $^{77}\text{Se}\{-^1\text{H}\}$  NMR: 33.9 ppm ( $^2J_{\text{Se-Y}} = 6$  Hz;  $^1J_{\text{Se-P}} = 581$  Hz).  $^{89}\text{Y}\{-^1\text{H}\}$  NMR: 436 ppm (t,  $^2J_{\text{Y-P}} = 5$  Hz). No absorption is present in the UV/vis spectrum between 230 and 800 nm.

**X-ray Crystallography.** A clear, colorless thin block of **1** or **2** was isolated under immersion oil in an  $\text{N}_2$ -filled crystal mounting box and suspended in a Nylon loop before being quickly frozen in the dry  $\text{N}_2$  stream of a Bruker Smart CCD diffractometer for data collection. Data for both compounds were collected at -120 °C with the use of graphite-monochromatized Mo K $\alpha$  radiation ( $\lambda = 0.71073$  Å). Final unit cell dimensions were obtained from 8192 reflections tallied during data processing. Data collections in  $\omega$  scan mode were performed with the program SMART.<sup>22</sup> Cell refinement and data reduction were made with the program SAINT<sup>22</sup> and face-indexed numerical absorption corrections were applied with the program XPREP.<sup>22</sup> The program SADABS was also applied to address incident beam anomalies (possible crystal decay,

**Table 1.** Crystal Data and Structure Refinement for  $\text{Y}[\eta^3\text{-N}(\text{SPPH}_2)_2]_3$  (**1**) and  $\text{Y}[\eta^3\text{-N}(\text{SePPh}_2)_2]_2[\eta^3\text{-N}(\text{SePPh}_2)_2]\cdot\text{CH}_2\text{Cl}_2$  (**2**)

	<b>1</b>	<b>2</b>
chemical formula	$\text{C}_{72}\text{H}_{60}\text{N}_3\text{P}_6\text{Se}_6\text{Y}$	$\text{C}_{72}\text{H}_{60}\text{N}_3\text{P}_6\text{Se}_6\text{Y}\cdot\text{CH}_2\text{Cl}_2$
fw	1434.32 <sup>a</sup>	1800.65
space group	$R\bar{3}c$	$P2_1/n$
<i>a</i> (Å)	14.927(5)	13.3511(17)
<i>b</i> (Å)	14.927(5)	38.539(7)
<i>c</i> (Å)	56.047(13)	14.108(2)
$\alpha$ (°)	90	90
$\beta$ (°)	90	94.085(13)
$\gamma$ (°)	120	90
<i>V</i> , Å <sup>3</sup>	10815(6)	7241(2)
<i>d</i> <sub>calcd</sub> (g/cm <sup>3</sup> )	1.321 <sup>a</sup>	1.652
<i>T</i> , °C	-120	-120
<i>Z</i>	6	4
linear abs coeff (cm <sup>-1</sup> )	12 <sup>a</sup>	41
transm coeff	0.60–0.93	0.42–0.59
$R_1(F)^b$ ( $F_o^2 > 2\sigma(F_o^2)$ )	0.042	0.037
$R_w(F_o^2)^c$ (all data)	0.0908	0.0767

<sup>a</sup> This value ignores the ill-defined solvent molecules responsible for the residual electron density. <sup>b</sup>  $R_1(F) = \sum||F_o| - |F_c||/\sum|F_o|$ . <sup>c</sup>  $R_w(F_o^2) = [\sum w(F_o^2 - F_c^2)^2/\sum wF_o^4]^{1/2}$ ;  $w^{-1} = \sigma^2(F_o^2) + (0.04F_o^2)^2$  for  $F_o^2 \geq 0$ ;  $w^{-1} = \sigma^2(F_o^2)$  for  $F_o^2 \leq 0$ .

incident beam absorption, and different generator settings among frames) through the assignment of individual scale factors for each frame and the smoothing of them with a seven-point quadratic Savitsky–Golay filter.<sup>22</sup> The structures were solved by standard Patterson methods and refined by full-matrix least-squares methods.<sup>23</sup> During refinement of **1** there remained significant residual electron density near the  $\bar{3}$  axis (Wyckoff site 6b). This density could not be modeled adequately. Accordingly, the program SQUEEZE<sup>24</sup> in the PLATON<sup>25</sup> suite of programs was used to handle this problem. Electron density totaling 220 e<sup>-</sup> per unit cell was found; this translates to approximately one  $\text{CH}_2\text{Cl}_2$  molecule per metal complex. This presumed  $\text{CH}_2\text{Cl}_2$  molecule, however, is lost upon isolation or analysis because the chemical analysis corresponds to that for the unsolvated species. Compound **2** crystallizes from concentrated  $\text{CH}_2\text{Cl}_2$  solutions having one ordered  $\text{CH}_2\text{Cl}_2$  molecule per Y center. The final models involved anisotropic displacement parameters for all non-hydrogen atoms and were refined to  $R_1(F)$  values of 0.042 (**1**) and 0.037 (**2**) for those data having  $F_o^2 > 2\sigma(F_o^2)$ . Although the positions of some hydrogen atoms were found in difference electron density maps, all were ultimately generated in calculated positions and constrained with the use of a riding model. The isotropic displacement parameter for a given hydrogen atom was set 1.2 times larger than the displacement parameter of the atom to which it is attached. A structure determination of the ether solvate of  $\text{Y}[\text{N}(\text{SePPh}_2)_2]_3$  (**2a**) was carried out in a manner similar to that for compounds **1** and **2**. (Crystal data for  $\text{Y}[\text{N}(\text{SePPh}_2)_2]_3\cdot(\text{CH}_3\text{CH}_2)_2\text{O}$ :  $\text{C}_{72}\text{H}_{60}\text{N}_3\text{P}_6\text{Se}_6\text{Y}\cdot\text{C}_4\text{H}_{10}\text{O}$ , monoclinic,  $P2_1/n$ ,  $a = 21.545(4)$  Å,  $b = 13.894(3)$  Å,  $c = 24.760(5)$  Å,  $\beta = 95.17(3)^\circ$ ,  $V = 7381.7$  Å<sup>3</sup>,  $Z = 4$ .) Crystallographic data for **1** and **2** are listed in Table 1, and selected bond distances and angles for **1**, **2**, and **2a** are listed in Table 2. Further crystallographic details for all three structures may be found in Supporting Information.

## Results and Discussion

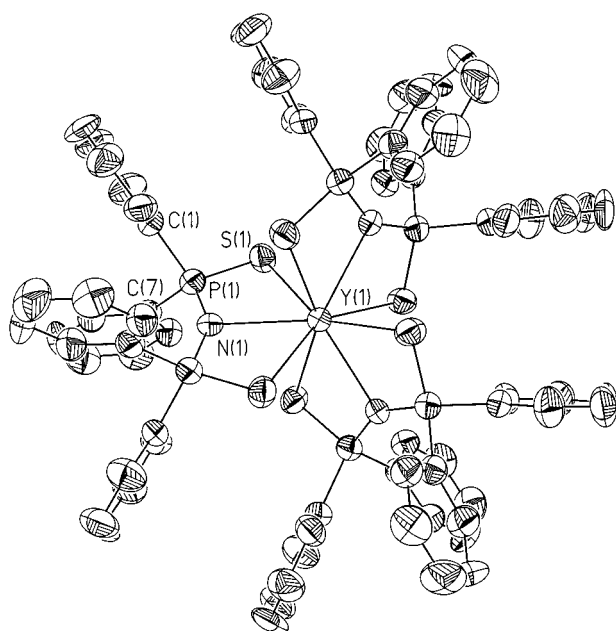
**Syntheses.** The reaction of a 3:1 stoichiometry of  $\text{HN}(\text{QPPH}_2)_2$  with  $\text{Y}[\text{N}(\text{SiMe}_3)_2]_3$  in  $\text{CH}_2\text{Cl}_2$  followed by concentra-

- (22) SMART Data Collection, version 5.054, and SAINT-Plus Data Processing Software for the SMART System, version 6.0; Bruker Analytical X-Ray Instruments, Inc.: Madison, WI, 1999.
- (23) Sheldrick, G. M. SHELXTL PC, An Integrated System for Solving, Refining, and Displaying Crystal Structures from Diffraction Data, version 5.0; Siemens Analytical X-Ray Instruments, Inc.: Madison, WI, 1994.
- (24) van der Sluis, P.; Spek, A. L. *Acta Crystallogr., Sect. A: Found. Crystallogr.* **1990**, *46*, 194–201.
- (25) Spek, A. L. *Acta Crystallogr., Sect. A: Found. Crystallogr.* **1990**, *46*, C34.

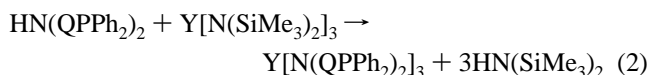
**Table 2.** Selected Bond Distances (Å) and Angles (deg) for  $Y[\eta^3\text{-N}(\text{SPPH}_2)_2]_3$  (**1**),  $Y[\eta^2\text{-N}(\text{SePPH}_2)_2]_2[\eta^3\text{-N}(\text{SePPH}_2)_2] \cdot \text{CH}_2\text{Cl}_2$  (**2**), and  $Y[\eta^2\text{-N}(\text{SePPH}_2)_2]_2[\eta^3\text{-N}(\text{SePPH}_2)_2] \cdot \text{C}_4\text{H}_{10}\text{O}$  (**2a**)

	<b>1</b>	<b>2</b>	<b>2a<sup>b</sup></b>
Y(1)–Q(1) <sup>a</sup>	2.9130(11)	2.9063(8)	2.9749(11)
Y(1)–Q(2)		2.9427(8)	2.9479(12)
Y(1)–Q(3)		2.9096(8)	2.8798(13)
Y(1)–Q(4)		2.9109(7)	2.9328(11)
Y(1)–Q(5)		2.8816(8)	2.8909(13)
Y(1)–Q(6)		2.9163(7)	2.9516(13)
Y(1)–N(1)	2.560(4)	2.428(3)	2.409(5)
Q(1)–Y(1)–Q(2)	125.51(4)	131.96(2)	132.46(3)
Q(3)–Y(1)–Q(4)		87.110(17)	86.41(3)
Q(5)–Y(1)–Q(6)		88.736(18)	85.74(3)

<sup>a</sup> Q = S in **1**, and Q = Se in **2** and **2a**. Only the unique metrical information is given for compound **1**, which has crystallographically imposed symmetry 32. In **2** and **2a** the  $\eta^3$ -bound ligands contain Se(1) and Se(2) and the  $\eta^2$ -bound ligands contain the other Se atoms. <sup>b</sup> Further crystallographic data for **2a** are given in Supporting Information.

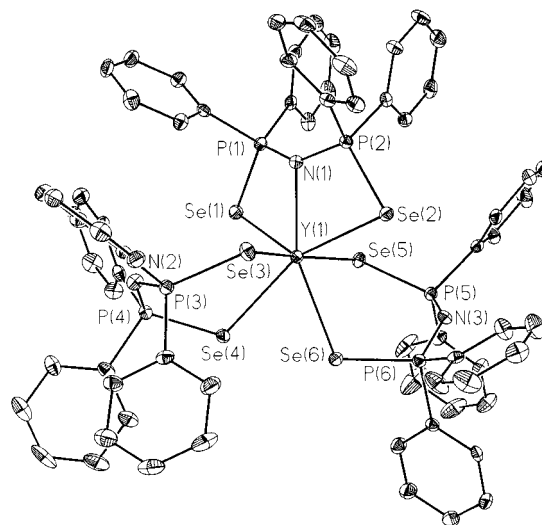
**Figure 1.** Structure of  $Y[\eta^3\text{-N}(\text{SPPH}_2)_2]_3$  (**1**). Anisotropic displacement parameters are drawn at the 80% probability level. Here and in Figure 2 hydrogen atoms have been omitted for the sake of clarity.

tion yields the colorless analytically pure compounds  $Y[\text{N}(\text{SPPH}_2)_2]_3$  (**1**) and  $Y[\text{N}(\text{SePPH}_2)_2]_3$  (**2**):



Isolated yields for the reactions were 79% and 91% for **1** and **2**, respectively. The compounds are soluble in THF and  $\text{CH}_2\text{Cl}_2$ ; they are unstable toward air and water but are stable under inert conditions and in air under oil for extended periods. Neither shows absorptions in the UV/vis spectrum above 300 nm. Crystals of **1** and **2** suitable for diffraction studies are easily grown from concentrated  $\text{CH}_2\text{Cl}_2$  solutions cooled to  $-15^\circ\text{C}$ . These crystals contain  $\text{CH}_2\text{Cl}_2$ . Very large crystals (often greater than 1 mm in length) can also be obtained from THF/pentane solutions, though these crystals are unstable out of solution.

**Structures.** Figure 1 shows the structure of  $Y[\text{N}(\text{SPPH}_2)_2]_3$  (**1**), and Figure 2 shows the structure of  $Y[\text{N}(\text{SePPH}_2)_2]_3$  (**2**) with the numbering schemes. Whereas compounds **1** and **2** both contain a Y atom chelated by three  $[\text{N}(\text{QPPH}_2)_2]^-$  ligands, the

**Figure 2.** Structure of  $Y[\eta^2\text{-N}(\text{SePPH}_2)_2]_2[\eta^3\text{-N}(\text{SePPH}_2)_2]$  (**2**). Anisotropic displacement parameters are drawn at the 50% probability level.

connectivity is not the same. In **1**, the metal is ligated  $\eta^3$  through two S atoms and an N atom to the three  $[\text{N}(\text{SPPH}_2)_2]^-$  ligands to make a formally nine-coordinate Y center ( $Y[\eta^3\text{-N}(\text{SPPH}_2)_2]_3$ ). In **2**, two of the three  $[\text{N}(\text{SePPH}_2)_2]^-$  ligands are coordinated  $\eta^2$  through the two Se atoms and one  $[\text{N}(\text{SePPH}_2)_2]^-$  ligand is coordinated  $\eta^3$  through the two Se atoms and an N atom to make a formally seven-coordinate Y center ( $Y[\eta^2\text{-N}(\text{SePPH}_2)_2]_2[\eta^3\text{-N}(\text{SePPH}_2)_2]$ ). The presumption is that in **1** the six smaller S atoms leave enough room for three additional N atoms from the ligand to coordinate whereas in **2** the six larger Se atoms leave only enough room for one N atom to coordinate. A similar steric argument was used to explain the molecular structure of  $\text{Cp}_2\text{Yb}[\eta^3\text{-N}(\text{SPPH}_2)_2]$  versus that of  $\text{Cp}_2\text{Yb}[\eta^2\text{-N}(\text{SePPH}_2)_2]$ .<sup>1</sup> However, in that earlier paper<sup>1</sup> we discussed possible steric and electronic effects in the bonding of the imidodiphosphinochalcogenido and imidodiphosphinoxido ligands to rare earths of varying sizes and noted that the steric argument just presented cannot explain the molecular structure of  $\text{Sm}[\eta^2\text{-N}(\text{SePPH}_2)_2][\eta^3\text{-N}(\text{SePPH}_2)_2](\text{THF})_2$  versus that of  $\text{Sm}[\eta^2\text{-N}(\text{SPPH}_2)_2]_2(\text{THF})_2$ .<sup>26</sup>

The geometry about the Y center in compounds **2** and **2a** may be described as a distorted pentagonal bipyramid with atoms Se(3) and Se(5) in the axial positions and atoms N(1), Se(1), Se(2), Se(4), and Se(6) in the equatorial positions. But note that there are some differences in detail (Table 2) that must result from "crystal packing forces", that is, from **2** being a  $\text{CH}_2\text{Cl}_2$  solvate and **2a** being a  $(\text{CH}_3\text{CH}_2)_2\text{O}$  solvate. The Se(3)–Y(1)–Se(5) angles are  $168.53(2)^\circ$  for **2** and  $174.47(3)^\circ$  for **2a**. The deviations of the N–P–N atoms of the  $\eta^3$ -bound ligand from the Y(1)–Se(1)–Se(2) plane are larger in **2** (N(1),  $-0.88$  Å; P(1),  $-0.83$  Å; P(2),  $-0.85$  Å) than in **2a** (N(1),  $-0.19$  Å; P(1),  $-0.18$  Å; P(2),  $-0.22$  Å). The Y–Se distances, (2.8816(8) to 2.9427(8) Å in **2** versus 2.8798(13) to 2.9749(11) Å in **2a**), differ in their grouping. As opposed to **2**, in **2a** the axial bonds are distinctly the shortest and are on average 0.07 Å less than the equatorial bonds. Surprisingly, the Y–S bond length of 2.9130(11) Å for **1** is very similar to the Y–Se bond lengths in **2** and **2a** (Table 2).

Structurally characterized rare-earth imidodiphosphinochalcogenido complexes are limited to some  $\text{Sm}(\text{II})$ <sup>26</sup> and  $\text{Cp}_2\text{Ln}$  species.<sup>1</sup> The Y–S distances in  $Y[\text{N}(\text{SPPH}_2)_2]_3$  (Table 2) are in

(26) Geissinger, M.; Magull, J. Z. *Anorg. Allg. Chem.* **1997**, 623, 755–761.

agreement with those in  $\text{Cp}_2\text{Y}[\text{N}(\text{SPPH}_2)_2]$  (2.9345(16) and 2.9278(19) Å)<sup>1</sup> (and somewhat surprisingly agree with the Yb–S distances in  $\text{Cp}_2\text{Yb}[\text{N}(\text{SPPH}_2)_2]$  (2.9400(6) and 2.8818(6) Å)<sup>1</sup>, given the difference in Yb(III) and Y(III) radii).<sup>27</sup> However, the Y–Se distances in  $\text{Y}[\text{N}(\text{SePPH}_2)_2]_3$  (Table 2) are shorter than those in  $\text{Cp}_2\text{Y}[\text{N}(\text{SePPH}_2)_2]$  (3.0524(18) and 3.0528(13) Å).<sup>1</sup> In  $\text{Sm}[\eta^2\text{-N}(\text{SePPH}_2)_2][\eta^3\text{-N}(\text{SePPH}_2)_2](\text{THF})_2$ , the Sm–Se distances for the  $\eta^3$ -bound ligand average 3.17(1) Å compared with that of 3.12(1) Å for the  $\eta^2$ -bound ligand;<sup>26</sup> however, in **2**,  $\text{Y}[\eta^2\text{-N}(\text{SePPH}_2)_2][\eta^3\text{-N}(\text{SePPH}_2)_2]$ , the Y–Se distances do not reflect differences in ligation. Of course, the Se–Y–Se bite angles of the  $\eta^2$ -bound ligands in **2** (average 87.9(8)°) are considerably smaller than those of the  $\eta^3$ -bound ligands in **2** (131.96(2)°) and **1** (125.51(4)°).

Since the structure of **1** possesses crystallographic symmetry  $D_3$  (32), the  $\text{YN}_3$  fragment is planar, the Y–N distances are equal, and the N–Y–N angles are 120°. The Y–N distance of 2.560(4) Å in **1** is longer than that in the structure of  $\text{Cp}_2\text{Y}[\eta^3\text{-N}(\text{SPPH}_2)_2]$  (2.431(3) Å)<sup>1</sup> where the ligand is similarly coordinated to the Y center. Surprisingly, in **2** and **2a** the Y–N bond distances of 2.428(3) and 2.409(5) Å do not differ significantly from the Y–N distance in **1** and are close to the Y–N bond distance in  $\text{Cp}_2\text{Y}[\text{N}(\text{SePPH}_2)_2]$  (2.449(5) Å).<sup>1</sup>

Although there are very few Y–Se distances in the literature for comparison, the Y–S and Y–N distances found here are decidedly longer than corresponding distances in compounds exhibiting covalent bonding. Thus, consider the Y–S distances in  $[(\text{Et}_3\text{CS})_2\text{Y}(\mu\text{-SCEt}_3\text{Py})_2]_2$  (terminal Y–S distances of 2.587(3) and 2.681(3) Å; bridging Y–S distances of 2.848(3) and 2.850(3) Å),<sup>28</sup> and the Y–N single bond distances in negatively charged N-containing species, such as  $\text{Y}[\text{N}(\text{SiMe}_3)_2]_3$ <sup>29</sup> (2.224(6) Å) and  $(\text{C}_6\text{H}_5\text{CN})_2\text{Y}[\text{N}(\text{SiMe}_3)_2]_3$ <sup>29</sup> (range 2.248(4) to 2.265(4) Å). Note also the sensitivity of the metal geometry in **2** and **2a** to the solvent of crystallization and the trends, or lack thereof, in Ln–Q distances in the present compounds. We conclude that the interaction of the hard Ln centers with the soft chalcogen atoms of these ligands is largely ionic in nature, but speculation beyond that is impossible given the limited structural data. Note that the question of covalent versus ionic bonding in rare-earth cyclopentadienyl complexes remains an open one,<sup>30</sup> despite a wealth of structural information.

The P–Q bond distances in compounds **1** (1.981(1) Å) and **2** (average 2.16(1) Å) are longer than those in the starting materials  $\text{HN}(\text{QPPH}_2)_2$  (Q = S, 1.937(1) and 1.950(1) Å;<sup>31</sup> Q = Se, 2.085(1) and 2.101(1) Å<sup>13</sup>); thus, a reduction in the P–Q bond order occurs upon deprotonation and coordination of the ligand to the metal center. There is no difference in the P–Q bond distances of the  $\eta^2$ - and  $\eta^3$ -bound ligands in **2** (average 2.146(7) and 2.169(7) Å, respectively). P–N distances in **1** (1.6101(15) Å) and **2** (average 1.61(2) Å) are the same and equal to those in the compounds  $\text{Cp}_2\text{Ln}[\text{N}(\text{QPPH}_2)_2]$  (average 1.62(1) Å).<sup>1</sup>

**NMR Studies.** With the general lack of solution studies of soluble rare-earth chalcogenide compounds,<sup>32–37</sup> the present

**Table 3.** Selected NMR Spectroscopic Data<sup>a</sup>

	<sup>31</sup> P	<sup>77</sup> Se	<sup>89</sup> Y	<sup>1</sup> J <sub>P–Se</sub>	<sup>2</sup> J <sub>P–Y</sub>	<sup>1</sup> J <sub>Se–Y</sub>
$\text{Y}[\text{N}(\text{SPPH}_2)_2]_3$ ( <b>1</b> )	42.5		284		4	
$\text{Y}[\text{N}(\text{SePPH}_2)_2]_3$ ( <b>2</b> )	32.4	33.9	436	581	5	6 <sup>b</sup>
$\text{HN}(\text{SPPH}_2)_2$	56.9					
$\text{HN}(\text{SePPH}_2)_2$	52.3	–163		790		
$\text{Cp}_2\text{Y}[\text{N}(\text{SPPH}_2)_2]$	47.8		–153		4	
$\text{Cp}_2\text{Y}[\text{N}(\text{SePPH}_2)_2]$	41.03	–127	–170	604	4	12

<sup>a</sup> Chemical shifts are in ppm. Coupling constants are in Hz. NMR data for the starting material and for  $\text{Cp}_2\text{Y}[\text{N}(\text{SPPH}_2)_2]$  and  $\text{Cp}_2\text{Y}[\text{N}(\text{SePPH}_2)_2]$  are taken from ref 1. <sup>b</sup> The <sup>1</sup>J<sub>Se–Y</sub> value of 6 Hz is approximate because the peak has unresolved shoulders (see NMR Studies).

compounds are attractive for NMR spectroscopic study because they contain, among others, <sup>31</sup>P, <sup>89</sup>Y, and <sup>77</sup>Se (for **2**) active nuclei. These data are summarized in Table 3.

The  $D_3$  symmetry of compound **1** in the solid-state structure is maintained in solution. <sup>31</sup>P NMR spectroscopy reveals a single resonance at 42.5 ppm from the six equivalent <sup>31</sup>P atoms. This resonance is shifted to lower frequency compared with that of the starting material (see Table 3). This peak is split into a doublet from two-bond P–Y coupling (<sup>2</sup>J<sub>P–Y</sub> = 4 Hz). This same 4 Hz coupling is seen in  $\text{Cp}_2\text{Y}[\eta^3\text{-N}(\text{SPPH}_2)_2]$ , which exhibits a similar shift of the resonance to lower frequencies.<sup>1</sup> A peak in the <sup>89</sup>Y NMR spectrum (<sup>89</sup>Y spin = 1/2, 100% abundant) for **1** at 284 ppm is shifted to lower frequency compared with the resonance at 563 ppm of the starting material,  $\text{Y}[\text{N}(\text{SiMe}_3)_2]_3$ .<sup>38</sup> The two-bond Y–P coupling to the six P atoms should produce a heptuplet, though this is not resolved. Rather, the peak is a broadened multiplet.

From the <sup>31</sup>P and <sup>77</sup>Se NMR spectra (see below) of compound **2**,  $\text{Y}[\eta^2\text{-N}(\text{SePPH}_2)_2][\eta^3\text{-N}(\text{SePPH}_2)_2]$ , we infer that a fluxional process occurs. Both spectra show broadened resonances for single <sup>31</sup>P and <sup>77</sup>Se atoms; thus, there is no distinction between  $\eta^2$ - and  $\eta^3$ -bound ligands. The <sup>31</sup>P NMR spectrum shows a single peak at 32.4 ppm with satellites arising from the coupling to the NMR-active <sup>77</sup>Se nuclei (<sup>77</sup>Se spin = 1/2, 7.8% abundant). Variable temperature <sup>31</sup>P NMR spectra from 15 to –40 °C show neither splitting of the resonance nor shift in its position. The value for <sup>1</sup>J<sub>P–Se</sub> of 581 Hz is typical for a deprotonated, metal-coordinated ligand (see Table 3 for other examples). The splitting in these satellites that would arise from two-bond P–P coupling manifests itself in an unresolved broadened multiplet at all temperatures.

The <sup>77</sup>Se NMR spectrum of **2** is shown in Figure 3. Since only one set of peaks is found in the spectrum, the discussion will assume that the Se atoms are averaged to one position as inferred from the <sup>31</sup>P NMR spectrum. The peak ( $\delta$  = 33.9 ppm) is found at higher frequency than the starting material ( $\delta$  = –163 ppm). It is also higher than that in  $\text{Cp}_2\text{Y}[\text{N}(\text{SePPH}_2)_2]$  ( $\delta$  = –127 ppm), which is affected by the shielding power of the Cp<sup>–</sup> rings attached to the Y center. The large splitting (580 Hz) corresponds to the <sup>1</sup>J<sub>P–Se</sub> splitting found in the <sup>31</sup>P NMR spectrum (see above). These peaks are subsequently split into doublets (6 Hz). Each individual peak appears to have shoulders.

(27) Shannon, R. D. *Acta Crystallogr., Sect. A: Cryst. Phys., Diff., Theor. Gen. Crystallogr.* **1976**, *32*, 751–767.

(28) Purdy, A. P.; Berry, A. D.; George, C. F. *Inorg. Chem.* **1997**, *36*, 3370–3375.

(29) Westerhausen, M.; Hartmann, M.; Pfitzner, A.; Schwarz, W. Z. *Anorg. Allg. Chem.* **1995**, *621*, 837–850.

(30) Sockwell, S. C.; Hanusa, T. P. *Inorg. Chem.* **1990**, *29*, 76–80.

(31) Husebye, S.; Maartmann-Moe, K. *Acta Chem. Scand., Ser. A* **1983**, *37*, 439–441.

(32) Cray, D. R.; Arnold, J. J. *Am. Chem. Soc.* **1993**, *115*, 2520–2521.

(33) Cary, D. R.; Ball, G. E.; Arnold, J. J. *Am. Chem. Soc.* **1995**, *117*, 3492–3501.

(34) Arnold, J. *Prog. Inorg. Chem.* **1995**, *43*, 353–417.

(35) Strzelecki, A. R.; Timinski, P. A.; Helsel, B. A.; Bianconi, P. A. *J. Am. Chem. Soc.* **1992**, *114*, 3159–3160.

(36) Strzelecki, A. R.; Likar, C. L.; Helsel, B. A.; Utz, T.; Lin, M. C.; Bianconi, P. A. *Inorg. Chem.* **1994**, *33*, 5188–5194.

(37) Takahashi, R.; Ishiguro, S.-I. *J. Chem. Soc., Faraday Trans. 2* **1992**, *88*, 3165–3170.

(38) This is to be compared with a value of 570.0 ppm recorded for a sample in CDCl<sub>3</sub> (Coan, P. S.; Hubert-Pfalzgraf, L. G.; Caulton, K. G. *Inorg. Chem.* **1992**, *31*, 1262–1267).

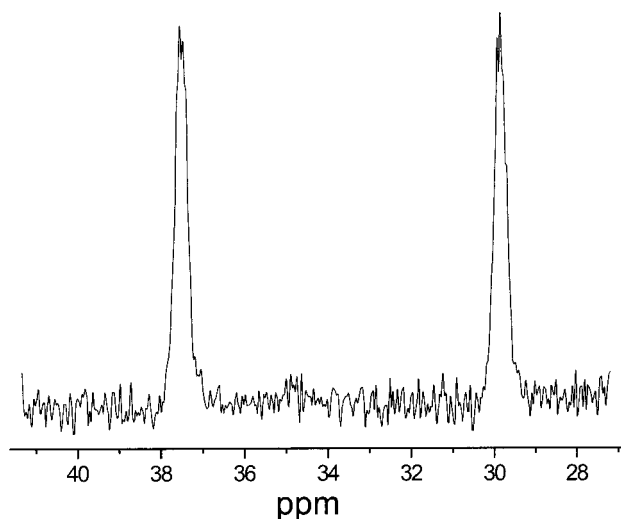


**Figure 3.**  $^{77}\text{Se}$  NMR spectrum (shifts in ppm) of  $\text{Y}[\eta^2\text{-N}(\text{SePPh}_2)_2]_2\text{-}[\eta^3\text{-N}(\text{SePPh}_2)_2]$  (**2**). Collection parameters are listed in Experimental Section.

The 6 Hz coupling is half what would be expected from  $^1J_{\text{Se-Y}}$  coupling in an  $\eta^3$ -bound ligand (for example, the value for  $\text{Cp}_2\text{Y}[\text{N}(\text{SePPh}_2)_2]$  is  $^1J_{\text{Se-Y}} = 12$  Hz),<sup>1</sup> though with the unresolved shoulders a more accurate assignment of the coupling is not possible.

The  $^{89}\text{Y}$  NMR spectrum of **2** (Figure 4) contains a single resonance at 436 ppm that is split into a triplet of 5 Hz. The position of the shift is between that of the starting material (563 ppm) and that of the sulfide analogue (284 ppm; see Table 3). The coupling probably arises from two-bond Y–P coupling to the two P atoms of the  $\eta^3$ -bound ligand ( $^2J_{\text{Y-P}} = 5$  Hz). This assignment of the spectrum implies that both the Se and P atoms in the three ligands are exchanging between the  $\eta^2$ - and  $\eta^3$ -bound ligands (as we also infer from the  $^{31}\text{P}$  and  $^{77}\text{Se}$  NMR spectra) and that on average there is only one ligand attached  $\eta^3$  to the metal center, as in the solid-state structure. One expects the two-bond Y–P coupling from the  $\eta^2$ -bound ligand to be negligible, since electron delocalization between the P and Y atoms should be much less when the path from the Y to the P

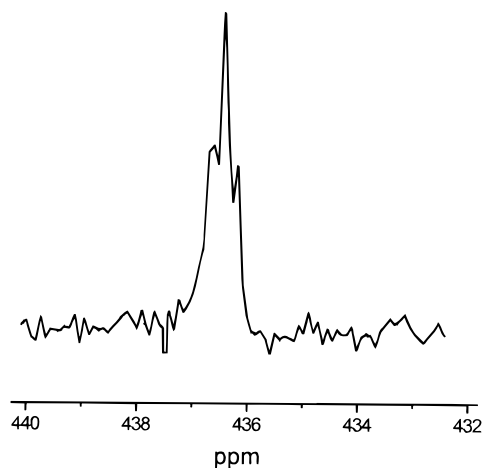


**Figure 4.**  $^{89}\text{Y}$  NMR spectrum (shifts in ppm) of  $\text{Y}[\eta^2\text{-N}(\text{SePPh}_2)_2]_2\text{-}[\eta^3\text{-N}(\text{SePPh}_2)_2]$  (**2**). Collection parameters are listed in Experimental Section.

is restricted to going through only the Se atom and not also through the N atom. Then the Y atom would see on average only two P atoms with appreciable coupling. The two-bond Y–P coupling would then produce a triplet. The coupling value of 5 Hz is similar to the coupling in  $\text{Cp}_2\text{Y}[\eta^3\text{-N}(\text{SePPh}_2)_2]$ <sup>1</sup> ( $^2J_{\text{Y-P}} = 4$  Hz; see Table 3), which further supports this as being coupling from an  $\eta^3$ -bound ligand. Y–Se coupling is not detected. Nevertheless, the solid-state and solution structures of  $\text{Y}[\eta^2\text{-N}(\text{SePPh}_2)_2]_2[\eta^3\text{-N}(\text{SePPh}_2)_2]$  (**2**) are the same.

**Acknowledgment.** This research was kindly supported by the National Science Foundation, Grant CHE-9819385.

**Supporting Information Available:** X-ray crystallographic files in CIF format for the structure determinations of  $\text{Y}[\eta^3\text{-N}(\text{SePPh}_2)_2]_3$  (**1**),  $\text{Y}[\eta^2\text{-N}(\text{SePPh}_2)_2]_2[\eta^3\text{-N}(\text{SePPh}_2)_2]\cdot\text{CH}_2\text{Cl}_2$  (**2**), and  $\text{Y}[\text{N}(\text{SePPh}_2)_2]_3\cdot(\text{CH}_3\text{CH}_2)_2\text{O}$  (**2a**). This material is available free of charge via the Internet at <http://pubs.acs.org>.

IC990984X